REPURPOSING PHARMACEUTICAL WASTE: EXPIRED MOLDAMIN AS A HIGH-EFFICIENCY, ECO-FRIENDLY CORROSION INHIBITOR FOR STEEL IN ACIDIC MEDIA

Ahmed A. KHATER[1,2,3,*], Norhan NADY[4], Narcis DUTEANU[3,5,*], Daniel-Marius DUDA-SEIMAN[6,*], M. M. EL-HALWANY[1,2], Mohamed S. SALEM[7,8]

This research evaluates the effectiveness of expired moldamin, a pharmaceutical waste material, as a corrosion inhibitor for AISI 1010 steel exposed to aqueous solutions of 1 M hydrochloric acid (HCl) and 1 M sulfuric acid (H_2SO_4) at 25 ± 2 °C. The study utilized electrochemical impedance spectroscopy (EIS) and potentiodynamic polarization (Tafel analysis) to assess corrosion behavior. Adsorption properties were investigated using the Langmuir adsorption isotherm, and thermodynamic activation parameters were analyzed to determine the spontaneity of the adsorption process. Results indicate that moldamin acts as a mixed-type inhibitor, providing notable protection through both anodic and cathodic mechanisms, with particularly strong performance in sulfuric acid. The highest inhibition efficiencies observed were 89.23% in HCl and 88.7% in H_2SO_4 at a concentration of 10^{-3} M. Surface characterization using 3D laser microscopy confirmed a marked decrease in surface roughness. Overall, the findings highlight moldamin's potential for both corrosion control and sustainable management of pharmaceutical waste.

[1] Department of Mathematics and Physics Engineering, Faculty of Engineering, Mansoura University, El-Mansoura, Egypt.
[2] Faculty of Engineering, Mansoura National University, El-Mansoura, Egypt
[3] Faculty of Chemical Engineering, Biotechnology and Environmental Protection, Politehnica University of Timisoara, Romania.
[4] Polymeric Materials Research Department, Advanced Technology and New Materials Research Institute
(ATNMRI), City of Scientific Research and Technological Applications (SRTA-City), Borg El-Arab City, Alexandria, Egypt
[5] National Institute for Research and Development in Electrochemistry and Condensed Matter Timisoara
[6] Department of Cardiology, "Victor Babes" University of Medicine and Pharmacy, Timisoara, Romania.
[7] Mechanical Power Engineering Department, Faculty of Engineering, Mansoura University, Mansoura, Egypt.
[8] Department of Mechanical and Industrial Engineering, College of Engineering, Majmaah University, Al-Majmaah, Saudi Arabia.
[*] Corresponding authors: Narcis Duteanu, e-mail: narcis.duteanu@upt.ro, Daniel-Marius Duda-Seiman, e-mail: daniel.duda-seiman@umft.ro, Ahmed A. Khater, e-mail: ahmedelawadi007@mans.edu.eg

Keywords: Moldamin; corrosion inhibition; AISI 1010 steel; Electrochemical impedance spectroscopy; 3D laser microscopy; Langmuir isotherm

1. Introduction

Corrosion is an inevitable degradation process that severely impacts metallic infrastructure in acidic environments. Low-carbon steels like AISI 1010 are prized in automotive, construction, and transportation for their mechanical properties and cost, yet they are highly susceptible to acidic corrosion. This leads to significant economic consequences from material loss, structural weakening, and high maintenance. Developing robust corrosion protection is therefore essential for extending the service life of steel infrastructure[1,2].

There are various techniques to protect metallic materials from corrosion, with the use of corrosion inhibitors being particularly favored due to their efficiency, simplicity of application, and cost-effectiveness [3,4]. Corrosion inhibitors are chemical agents that slow metal deterioration when added in small quantities to corrosive environments. Effective inhibitors are critical for enhancing the longevity of steel infrastructure. However, traditional inhibitors such as chromates and phosphates are toxic and environmentally hazardous, driving the need for safer, eco-friendly alternatives [5,6].

In recent years, attention has shifted increasingly to environmentally friendly and sustainable corrosion inhibitors derived from plant extracts, organic substances, and waste materials. Among these, pharmaceutical compounds (especially expired medications) have gained recognition as unconventional but promising corrosion inhibitors [7]. Although typically considered waste, expired pharmaceuticals contain complex molecular structures rich in heteroatoms such as oxygen, nitrogen, sulfur, and fluorine, as well as π-electrons, which enhance their ability to be adsorbed onto metal surfaces effectively [8,9]. Moldamin, characterized by its sulfur- and nitrogen-containing moieties, demonstrates high affinity for steel surfaces in acidic environments, enabling effective corrosion inhibition through surface complexation and electrochemical interaction [10,11]. Several studies have reported the effectiveness of antibiotics such as amoxicillin, paracetamol, and atorvastatin in mitigating corrosion in various metallic systems, demonstrating their potential as sustainable inhibitors [12–14].

Repurposing expired Moldamin also supports global sustainability by reducing chemical waste and promoting a circular economy. This study therefore not only assesses its corrosion protection but also contributes to waste valorization strategies for industrial use [15].

While pharmaceuticals show promise as corrosion inhibitors, research remains largely exploratory and limited to mild steel in HCl. Performance in other

environments, such as sulfuric acid on specific grades like AISI 1010 steel, is inadequately investigated.

This research therefore systematically assesses Moldamin as a cost-efficient, green inhibitor for AISI 1010 steel in acid. It characterizes its adsorption behavior, quantifies inhibition efficiency, and evaluates adherence to adsorption isotherms to determine its viability as a sustainable alternative.

2. Methodology

2.1. Materials

The corrosion behavior of AISI 1010 steel in hydrochloric acid (HCl, Riedel-de Haën, 37%) and sulfuric acid (H_2SO_4, Merck, p.a., 95-97%) solutions was investigated, along with the inhibitory efficacy of the expired pharmaceutical compound Moldamin (Moldamin, 1,200,000 IU per vial; Antibiotice S.A., Romania). Inhibitor concentrations ranging from 10^{-6} to 10^{-3} mol/L were employed. Moldamin ($C_{48}H_{56}N_6O_8S_2$) IUPAC name is (2S,5R,6R)-3,3-dimethyl-7-oxo-6-[(phenylacetyl)amino]-4-thia-1-azabicyclo [3.2.0] heptane-2-carboxylic acid benzathine (1:1), and the chemical structure is presented in Fig. 1.

The elemental composition was determined using optical emission spectrometry (Thermo Electron Corporation Genesys, Thermo Fisher Scientific, United States), and they are presented in Table 1

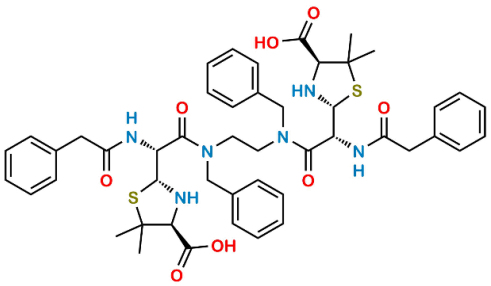

Fig. 1. Moldamin chemical structure

Table 1

Chemical composition of the AISI 1010 steel sample

Element	Fe	Cu	Mn	Si	C	Al	Cr	Mo
Wt%	98.82	0.483	0.372	0.1751	0.0941	0.067	0.06	0.030

2.2. Methods

2.2.1. Specimens' preparation

The preparation of AISI 1010 steel specimens for subsequent testing adhered to ASTM G1. The process commenced with mechanical polishing through a graded series of silicon carbide abrasive papers (120 to 2000 grit). Specimens were then subjected to ultrasonic cleaning in ethanol for contaminant removal,

followed by extensive rinsing in distilled water. After drying, specimens were stored in a desiccator to maintain surface integrity before testing.

2.2.2. Surface roughness

The samples were prepared under five distinct conditions: (1) polished AISI 1010 steel serving as the control, (2) after immersion in 1 M HCl,(3) after immersion in 1 M H_2SO, (4) following immersion in 1 M HCl containing 10^{-3} M Moldamin; and (5) following immersion in 1 M H_2SO_4 containing 10^{-3} M Moldamin.

Surface roughness was evaluated using a laser scanning three-dimensional measuring microscope (LEXT OLS 4000, Olympus, Japan). Initial two-dimensional surface images were acquired, followed by three-dimensional surface profiling using a 405 nm laser source.

2.2.3. Electrochemical measurements

The linear polarization (Tafel method) and electrochemical impedance spectroscopy (EIS) [16] were employed to investigate and highlight the corrosion-inhibiting properties of Moldamin on AISI 1010 steel. The experimental setup used a conventional 75 mL glass cell with a four-electrode configuration, connected to an AUTOLAB PGSTAT 302N potentiostat. The system included two graphite counter electrodes, an AISI 1010 steel working electrode, and a saturated Ag/AgCl reference electrode (Fig. 2), ensuring stable current distribution and measurement accuracy. Before each experiment, the working electrode surface was polished to achieve a uniform surface using different sandpapers of varying grit sizes to achieve a smooth finish, then thoroughly cleaned to remove any residual particles or contaminants and rinsed with distilled water to remove impurities, ensuring it was suitable for accurate electrochemical testing and corrosion studies.

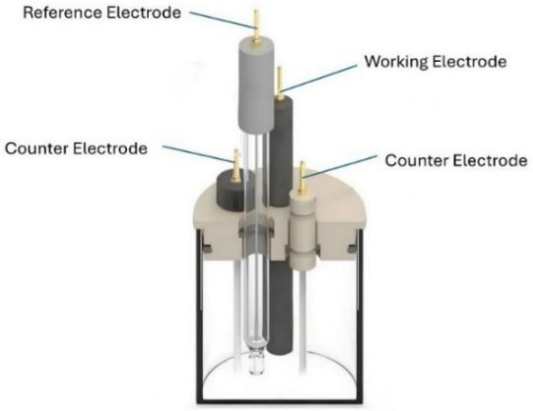

Fig. 2. Schematic diagram of cell configuration

Following this preparation, the electrode's potential stabilized for 45 minutes to ensure equilibrium and reliable measurement conditions. Linear polarization tests were performed at 1 mV/s (±250 mV vs. OCP) under quasi-stationary conditions at 25 °C. Measurements included uninhibited solution and Moldamin concentrations from 10^{-6} to 10^{-3} M, with triplicate trials/concentration. Tafel curves were then extrapolated to estimate the values of polarization parameters such as corrosion potential (Ecorr), corrosion current density (icorr), and corrosion rate (CR). From such parameters, the inhibition efficiency (IE) could also be estimated from Eq. 1 [16] as follows.

$$IE(\%) = \frac{i_{corr}^{o} - i_{corr}^{inh}}{i_{corr}^{o}} * 100 \quad (1)$$

Where: i_{corr}^{o} is the current density in the absence of Moldamin[μA/cm²]; i_{corr}^{inh} is the current density in the presence of Moldamin[μA/cm²].

EIS measurements were conducted using a Metrohm Autolab PGSTAT 302N potentiostat at the open circuit potential (OCP). Spectra were acquired over a frequency range of 0.01 Hz to 100 kHz with a 10 mV AC perturbation. Data from three repeated tests (n=3) were modeled in Nova 2.1.7 software using the equivalent circuit shown in Fig. 3, which consists of solution resistance (Rs) in series with a parallel constant phase element (CPE) and polarization resistance (Rp). The composite R_p encompasses the contributions of charge transfer resistance (R_{ct}), double-layer dispersion resistance (R_d), inhibitor-derived surface film resistance (R_f), and adsorption-mediated accumulation resistance (R_a) [17–19].

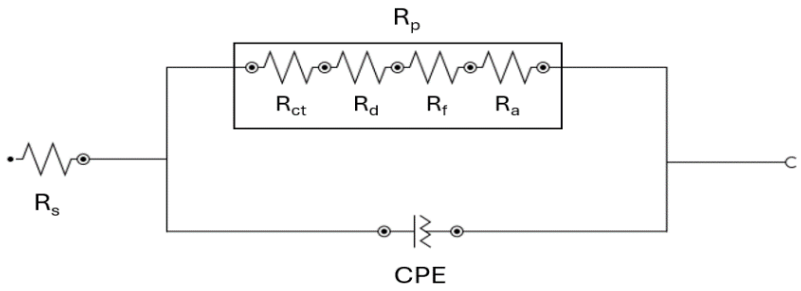

Fig. 3. Equivalent circuit used for simulation of data

To model the capacitance associated with depressed Nyquist semicircles, a constant-phase element (CPE), representing a non-ideal capacitor, replaces the pure capacitor in the circuit model. Its impedance is defined by [20]

$$Z_{CPE} = \frac{1}{Y_o(j\boldsymbol{\omega})^n} \quad (2)$$

Where: Z_{CPE} : the impedance of CPE; Y_o : the CPE coefficient (representing admittance, the reciprocal of impedance); ω : the angular frequency given by ω=2*π*f (having units in rad/s); n: A dimensionless parameter (0≤n≤1) that describes the degree of non-ideality:

The double-layer capacitance (C_{dl}) can be evaluated as follows

$$C_{dl} = \frac{Y_o \boldsymbol{\omega}^{n-1}}{\sin\left(n\left(\frac{\pi}{2}\right)\right)} \quad (3)$$

Where: $\boldsymbol{\omega}$ is given by:

$$\boldsymbol{\omega}_{max} = 2*\pi*f_{max} \quad (4)$$

corresponding to the peak frequency of the negative imaginary impedance component ($-Z_{imag}$).

Then, the inhibition efficiency can be calculated from another perspective using polarization resistance (Rp) as follows [16].

$$IE(\%) = \frac{R_P^{inh} - R_P^0}{R_P^{inh}} * 100 \quad (5)$$

Where: R_P^{inh} is the polarization resistance in the presence of Moldamin [Ω]; R_P^0 : is the polarization resistance in the absence of Moldamin [Ω].

2.2.4. Adsorption isotherms

Adsorption isotherms provide fundamental insights into how inhibitors interact with the AISI 1010 steel surface, explaining the corrosion inhibition mechanism. This adsorption process depends critically on the inhibitor's molecular structure, its charge distribution, and the nature of the charged metal surface and acidic media [17].

The surface coverage calculated using Eq. 6

$$\theta = \frac{CR^o - CR^{inh}}{CR^o} \quad (6)$$

Where: CR^o : the corrosion rate of steel in the absence of Moldamin [mm/year]; CR^{inh} : the corrosion rate of steel in the presence of Moldamin [mm/year].

The Langmuir adsorption isotherm is applied as in Eq.7 [17]

$$\frac{C_{inh}}{\theta} = C_{inh} + \frac{1}{k_{ads}} \quad (7)$$

Where: C_{inh} is the concentration of the inhibitor; θ is the surface coverage calculated from Eq. 6; K_{ads} is the adsorption constant, obtained from the intercept of the straight line, relates to the standard free energy of adsorption in Eq. 8 [21].

$$\Delta G_{ads}^0 = -RTln(55.5\, K_{ads}) \quad 8)$$

Where: R: is the universal gas constant [J/M. K]; T : is the absolute temperature[K].

3. Results and discussion

3.1. Linear polarization

Tafel curves shown in Fig. 4 and polarization parameters for AISI 1010 steel corrosion in both acid media, 1 M HCl and 1 M H_2SO_4, i.e., corrosion potential (E_{corr}), corrosion current density (i_{corr}), and corrosion rate (CR) were determined by

extrapolating the Tafel curves. Inhibition efficiency (IE%, Eq. 1) was calculated; results are presented in Table 2.

Tafel polarization confirms the high inhibition efficiency of Moldamin for AISI 1010 steel in 1 M HCl and H_2SO_4, which increases with concentration up to a maximum at 10^{-3} M. This concentration-dependent behavior indicates greater surface coverage by Moldamin molecules, approaching monolayer adsorption at optimal concentration.

Notably, the Tafel curves show a parallel shift of both anodic and cathodic branches, indicating that Moldamin acts as a mixed-type inhibitor. This implies that it concurrently suppresses the anodic dissolution of iron ($Fe \rightarrow Fe^{2+} + 2e^-$) and the cathodic hydrogen evolution reaction ($2H^+ + 2e^- \rightarrow H_2$). Such dual inhibition points to effective surface interaction with active corrosion sites.

Moldamin's similar inhibition in both HCl and H_2SO_4 underscores its versatility, indicating an anion-independent mechanism. This likely results from strong adsorption via both chemisorption—through donor-acceptor interactions—and physisorption. These findings confirm its strong potential as a robust, broad-spectrum acidic corrosion inhibitor.

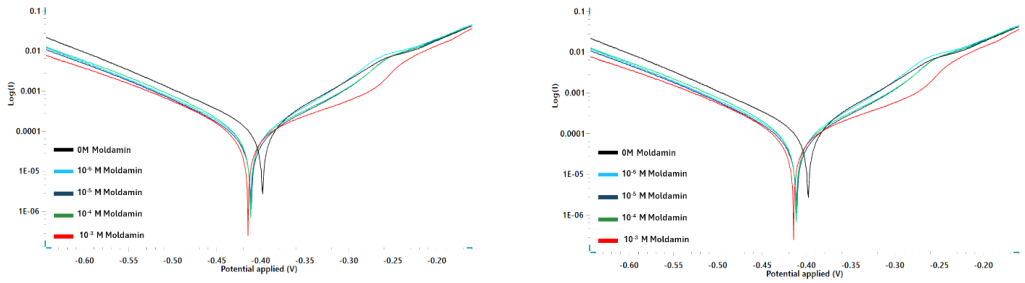

(a) (b)

Fig. 4 Tafel curves on AISI 1010 steel electrode in (a) 1 M HCL and (b) 1 M H_2SO_4 in the absence/presence of the moldamin.

As shown in Table 2, Tafel polarization data confirms Moldamin's concentration-dependent inhibition on AISI 1010 steel. In 1M HCl, i_{corr} decreased from 142.06 to 15.30 µA/cm² (89.23% efficiency), while in 1M H_2SO_4, it dropped from 361.76 to 43.42 µA/cm² (88.70% efficiency) at the optimal 10^{-3} M concentration.

The minimal Ecorr shifts (less than 30 mV) in both media confirm Moldamin acts as a mixed-type inhibitor [22], affecting both anodic and cathodic reactions. The moderate cathodic shifts (from -397.91 to -414.36 mV in HCl and from -387.87 to -395.51 mV in H_2SO_4) suggest a slightly greater influence on the cathodic process.

The corrosion penetration rate (CR) underscores Moldamin's practical efficacy. In 1M HCl, vcorr was reduced from 1.6507 to 0.17772 mm/year (89.2%

reduction). Even in the more aggressive H_2SO_4, it was lowered from 4.2048 to 0.5046 mm/year. These final rates are well below typical industrial thresholds, confirming its practical applicability in both environments.

Despite H_2SO_4 being a more aggressive environment than HCl, Moldamin achieves remarkably consistent and high inhibition efficiencies (~89% in HCl and ~89% in H_2SO_4). This anion-independent performance demonstrates a robust inhibition mechanism, making it a versatile and promising candidate for various acidic industrial applications.

Table 2

Polarization parameters for an AISI 1010 steel rod's corrosion process in an acid solution in the presence and absence of Moldamin.

Media	Moldamin Conc. (M)	E_{corr} (mV)	i_{corr} (μA/cm²)	CR (mm/year)	IE %	θ
HCL	0	-397.91	142.06	1.6507	0.00	0
	10^{-6}	-411.66	50.99	0.59255	64.10	0.641
	10^{-5}	-410.92	37.53	0.43613	73.58	0.7358
	10^{-4}	-411.38	20.11	0.23369	85.84	0.8584
	10^{-3}	-414.36	15.30	0.17772	89.23	0.8923
H_2SO_4	0	-387.87	361.76	4.2048	0.00	0
	10^{-6}	-408.72	154.03	1.7898	57.43	0.5743
	10^{-5}	-391.54	128.23	1.4911	66.60	0.666
	10^{-4}	-390.38	74.66	0.8675	80.57	0.8057
	10^{-3}	-395.51	43.42	0.5046	88.70	0.887

3.2. Electrochemical impedance spectroscopy

Nyquist plots (Fig. 5) show the EIS behavior of AISI 1010 steel in 1 M HCl and H_2SO_4 with and without Moldamin. All spectra display a single, depressed capacitive loop, indicative of a charge transfer-controlled process. The diameter of this semicircle, corresponding to the charge transfer resistance (Rct), increased markedly with inhibitor concentration in both acids.

This systematic increase in Rct, reaching a maximum at 10^{-3} M, demonstrates a concentration-dependent inhibition effect. The trend confirms that Moldamin adsorbs onto the steel surface, forming a protective film that impedes charge transfer. Although R_{ct} values were slightly lower in H_2SO_4, the inhibitor's strong performance in both media suggests effective adsorption via donor-acceptor interactions between its heteroatoms (N, O) and the iron surface. The non-ideal semicircles are attributed to surface heterogeneities common in inhibitor studies [23].

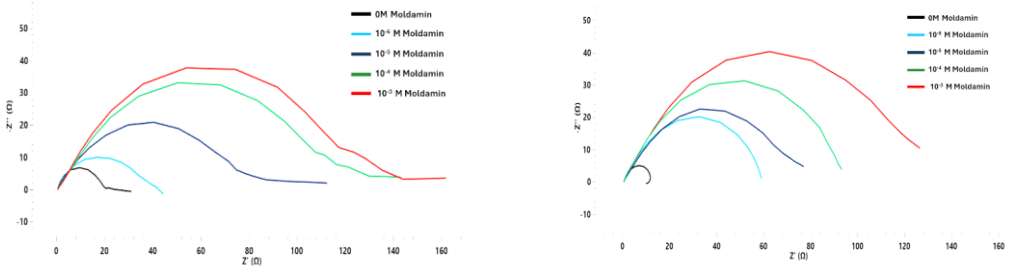

(a) (b)

Fig. 5. Nyquist plot for AISI 1010 steel electrode in (a)1 M HCL, (b)1 M H_2SO_4 in the absence/presence of Moldamin

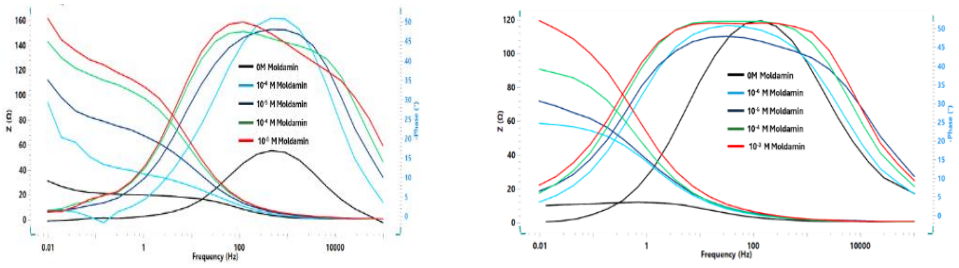

(a) (b)

Fig. 6. Bode plot for AISI 1010 steel electrode in (a)1 M HCL, (b)1 M H_2SO_4 in the absence/presence of Moldamin

Bode plots (Fig. 6) show the frequency response of AISI 1010 steel in uninhibited and Moldamin-inhibited 1 M HCl and H_2SO_4. In both acids, |Z| values increased significantly at low frequencies (0.01–1 Hz) with inhibitor concentration, reaching a maximum at 10^{-3} M, indicating enhanced barrier resistance from adsorbed Moldamin.

Phase angle curves broadened and shifted toward more negative values with concentration, reflecting formation of a more capacitive, protective surface film. Although absolute impedance was lower in H_2SO_4, the consistent trends—including intensified phase angle peaks approaching 50° and near-linear |Z| slopes—confirm effective inhibitor adsorption and transition toward diffusion-controlled behavior in both media [24].

Table 3

Electrochemical impedance parameters for an AISI 1010 steel rod's corrosion process in an acid solution in the presence and absence of Moldamin.

Media	Moldamin Conc. (M)	R_s (Ω)	C_{dl} (μF cm^{-2})	R_p (Ωcm^2)	IE %
	0	0.5903	113.956	20.963	0.00
	10^{-6}	0.6664	88.778	37.965	44.78

HCL	10^{-5}	0.8954	73.341	77.64	73.00
	10^{-4}	1.4068	55.055	112.16	81.31
	10^{-3}	1.6392	40.155	123.44	83.02
H_2SO_4	0	0.87518	128.875	22.496	0.00
	10^{-6}	1.3749	87.417	59.331	62.08
	10^{-5}	1.5429	71.858	71.551	68.56
	10^{-4}	1.4113	50.858	94.259	76.13
	10^{-3}	1.5953	37.375	126.44	82.21

The electrochemical impedance spectroscopy (EIS) results presented in Table 3 reveal significant changes in the impedance parameters of AISI 1010 steel in both 1 M HCl and 1 M H_2SO_4 media upon the addition of varying concentrations of Moldamin. In both acidic environments, a marked increase in polarization resistance (Rp) was observed with increasing inhibitor concentration, indicating a strong corrosion-inhibiting effect. Specifically, Rp increased from 20.96 $\Omega \cdot cm^2$ (blank solution) to 123.44 $\Omega \cdot cm^2$ in 1 M HCl, and from 22.50 $\Omega \cdot cm^2$ to 126.44 $\Omega \cdot cm^2$ in 1 M H_2SO_4, upon the addition of 10^{-3} M Moldamin. This trend suggests that Moldamin forms a protective film on the steel surface, effectively impeding the charge transfer process responsible for corrosion.

Concomitantly, the double-layer capacitance (C_{dl}) showed a substantial decrease as the inhibitor concentration increased. In the case of 1 M HCl, C_{dl} dropped from 113.96 $\mu F \cdot cm^{-2}$ to 40.15 $\mu F \cdot cm^{-2}$, while in 1 M H_2SO_4, it decreased from 128.88 $\mu F \cdot cm^{-2}$ to 37.38 $\mu F \cdot cm^{-2}$. The reduction in C_{dl} is indicative of the adsorption of Moldamin molecules onto the steel surface, displacing water molecules and reducing the local dielectric constant. This behavior points to the formation of a more compact and less permeable inhibitor layer, which effectively suppresses the corrosion reaction.

Furthermore, the inhibition efficiency (IE%) progressively improved with higher Moldamin concentrations, reaching 83.02% in 1 M HCl and 82.21% in 1 M H_2SO_4 at 10^{-3} M. These results confirm that Moldamin acts as a highly effective corrosion inhibitor in both media, likely through a mixed-type inhibition mechanism involving adsorption on both anodic and cathodic sites. Overall, the EIS data support the conclusion that Moldamin offers substantial protective performance against acid-induced corrosion of AISI 1010 steel, with optimal inhibition efficiency achieved at the highest tested concentration[25]. The overall trends observed in both the impedance modulus and phase angle plots are consistent with the characteristic response of mixed-type corrosion inhibitors such as Moldamin, which simultaneously suppress anodic metal dissolution and cathodic hydrogen evolution. This dual inhibition behavior reinforces the notion that Moldamin not only mitigates the rate of corrosion but also modifies the

electrochemical interface of the steel surface, leading to conditions that are less favorable for corrosion processes to occur.

3.3. Adsorption Isotherm

Fig. 7 shows a linear relationship between $\frac{C_{inh}}{\theta}$ and C_{inh} with a slope near unity, indicating that the inhibitor follows the Langmuir adsorption model described by Eq. 7.

The literature reports that ΔG^0_{ads} values of approximately -20 kJ/mol are characteristic of physical adsorption, whereas values near -40 kJ/mol imply chemical adsorption[26]. The adsorption behavior of Moldamin on AISI 1010 steel in 1 M HCl and 1 M H_2SO_4 media was evaluated using the Langmuir isotherm model. Excellent linear fits (R^2 = 0.99981 in HCl and 0.9999 in H_2SO in C_{inh}/θ versus C_{inh} plots validate Langmuir adsorption. The behavior implies monolayer inhibitor coverage with homogeneous adsorption sites. The calculated adsorption equilibrium constants K_{ads} were 4.13 × 10^5 M^{-1} in HCl and 1.93 × 10^5 M^{-1} in H_2SO_4, indicating stronger adsorption in the hydrochloric medium. Standard free energy of adsorption ΔG^0_{ads} was calculated according to Eq. 8 yielding values of –44.5 kJ/mol for HCl and –40.1 kJ/mol for H_2SO_4. These negative and large values (more negative than –40 kJ/mol) suggest that the adsorption process is spontaneous and predominantly chemical in nature (chemisorption). The stronger interaction in HCl may be attributed to enhanced electrostatic attraction between the protonated inhibitor species and the negatively charged steel surface in chloride-containing media.

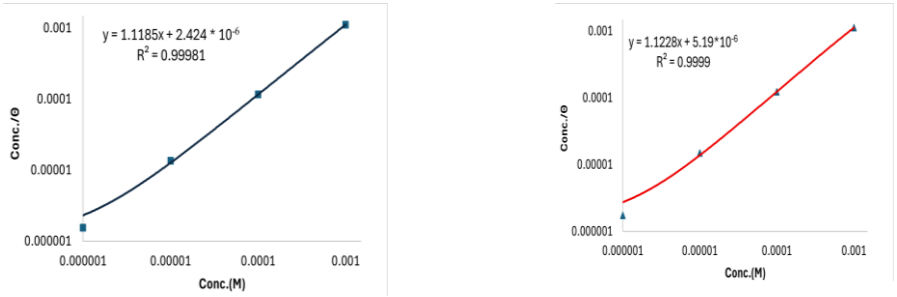

(a) (b)

Fig. 7. Langmuir adsorption isotherm plots for AISI 1010 steel at different concentrations of Moldamin in (a) 1 M HCl, and (b) 1 M H_2SO_4 media

3.4. Surface Characterization

The roughness, height, and valley values for all the samples were calculated from the images obtained shown in Fig. 8. Table 4 presents the surface roughness parameters: average roughness (Sa), root mean square roughness (Sq),

maximum peak height (Sp), maximum valley depth (Sv), and maximum height (Sz).

Table 4 presents the calculated surface roughness parameters for AISI 1010 steel samples subjected to different corrosive environments with and without Moldamin. Sample (a), representing the uncorroded or reference surface, exhibits the lowest values across all parameters, with Sa of 0.278 μm and Sz of 24.036 μm, indicating a relatively smooth and unperturbed surface.

In the case of Sample (b), which corresponds to steel exposed to 1 M HCl without any inhibitor, all roughness metrics increased significantly. The values of Sa (0.427 μm), Sp (45.441 μm), and Sz (74.744 μm) point to severe surface degradation, consistent with aggressive corrosion activity induced by hydrochloric acid. This surface damage is further supported by the high Sv value (32.155 μm), suggesting pronounced pitting or valley formation due to localized corrosion.

Upon the addition of 10^{-3} M Moldamin in HCl (Sample c), the roughness parameters notably decreased compared to the uninhibited HCl sample. For instance, Sa reduces to 0.418 μm and Sz to 47.539 μm, reflecting the protective influence of Moldamin. The lower Sp and Sv values (30.875 μm and 10.657 μm, respectively) confirm that the inhibitor effectively mitigates both peak growth and valley formation, likely through adsorption and barrier film formation on the steel surface.

A similar trend is observed in sulfuric acid media. Sample (d), exposed to 1 M H_2SO_4 alone, exhibits significant roughening with Sa of 0.476 μm and a maximum Sz of 72.176 μm, indicating strong corrosive attack. However, the introduction of 10^{-3} M Moldamin in this medium (Sample e) results in substantial surface smoothing. While Sa increases slightly to 0.548 μm due to residual roughness, the reduction in Sp and Sv (33.466 μm and 20.112 μm, respectively) compared to Sample (d) demonstrates Moldamin's inhibitory action in sulfuric acid, reducing both metal dissolution and surface deterioration.

Table 4

Electrochemical impedance parameters for AISI 1010 steel corrosion process in acid solution in the presence and absence of Moldamin.

Sample	S_a [μm]	S_q [μm]	S_p [μm]	S_v [μm]	S_z [μm]
(a)	0.277667	0.388333	19.00733	5.028667	24.036
(b)	0.427	0.579	45.441	32.155	74.744
(c)	0.418	0.531	30.875	10.65633	47.53933
(d)	0.476	0.672	41.689	35.447	72.176
(e)	0.548	0.684	33.466	20.112	53.578

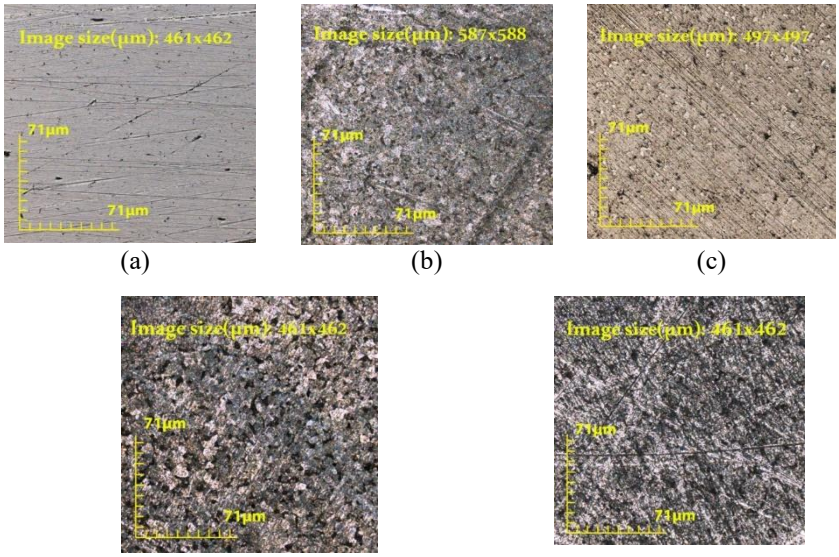

Fig. 8. 3-D laser microscopy surface analysis of AISI 1010 steel of (a) polished AISI 1010 steel, (b) post-immersion in 1M HCl, (c) 1M HCl + 10^{-3} M, (d) post-immersion in 1M H_2SO_4, and (e) 1M H_2SO_4 + 10^{-3} M Moldamin.

Overall, the surface roughness analysis supports the electrochemical data, confirming that Moldamin significantly reduces corrosion-induced topographical damage in both acidic environments, validating its role as an effective mixed-type inhibitor.

4. Conclusion

This study demonstrates that expired Moldamin is an effective and eco-friendly corrosion inhibitor for AISI 1010 steel in acidic media (1 M HCl and 1 M H_2SO_4). At 10^{-3} M concentration, the inhibitor achieved high efficiencies of 89.23% in HCl and 88.70% in H_2SO_4, as determined by both Tafel polarization and electrochemical impedance spectroscopy (EIS). The inhibitor exhibited a mixed-type mechanism, as indicated by parallel shifts in both anodic and cathodic Tafel branches, suppressing both iron dissolution ($Fe \rightarrow Fe^{2+} + 2e^-$) and hydrogen evolution ($2H^+ + 2e^- \rightarrow H_2$).

Adsorption of Moldamin onto the steel surface followed the Langmuir isotherm ($R^2 > 0.9998$), suggesting monolayer formation on a uniform surface. Thermodynamic parameters revealed spontaneous and predominantly chemical adsorption, with highly negative ΔG^0_{ads} values (–44.5 kJ/mol in HCl and –40.1 kJ/mol in H_2SO_4) and high adsorption equilibrium constants (K_{ads}= 4.13 × 10^5 M^{-1}

in HCl, 1.93×10^5 M^{-1} in H_2SO_4). These results point to strong donor-acceptor interactions between the inhibitor's heteroatoms (N, O, S) and the metal surface.

EIS measurements confirmed the formation of a protective barrier film, as evidenced by increased polarization resistance (Rp) and decreased double-layer capacitance (C_{dl}) with increasing inhibitor concentration. Surface roughness analysis using 3D laser microscopy further supported the electrochemical findings, showing reduced Sa and Sz parameters in inhibited samples compared to severely corroded controls.

Collectively, these findings establish expired Moldamin as a promising green corrosion inhibitor. Beyond its high efficacy, the repurposing of pharmaceutical waste aligns with circular economy principles, offering an environmentally sustainable approach to corrosion mitigation. Future research should address long-term durability, potential synergistic blends, and real-world application under industrial conditions.

REFERENCES

[1] A. Al-Amiery, W.N.R. Wan Isahak, W.K. Al-Azzawi, Sustainable corrosion Inhibitors: A key step towards environmentally responsible corrosion control, Ain Shams Engineering Journal 15 (2024) 102672. https://doi.org/https://doi.org/10.1016/j.asej.2024.102672.

[2] 1010 Steel: Properties and Key Applications – Metal Zenith, (n.d.). https://metalzenith.com/blogs/steel-properties/1010-steel-properties-and-key-applications (accessed July 2, 2025).

[3] G.E. Badea, A. Fodor, A.I.G. Petrehele, I. Maior, M. Toderaș, C.M. Morgovan, Evaluation of Phosphopolyoxometalates with Mixed Addenda (Mo, W, V) as Corrosion Inhibitors for Steels, Materials 16 (2023) 7600. https://doi.org/10.3390/ma16247600.

[4] A. Cojocaru, G.E. Badea, I. Maior, S. Dzitac, O.D. Stănășel, M. Sebeșan, C.D. Ionaș, P. Creț, Electrochemical Investigations of Galium verum Ethanolic Extract as a Steel Corrosion Eco-Inhibitor in the Acid Media: An Unexpected Versatility of Plant Chemistry, Materials 18 (2025) 2078. https://doi.org/10.3390/ma18092078.

[5] G. Broussard, O. Bramanti, F.M. Marchese, Occupational risk and toxicology evaluations of industrial water conditioning, Occup Med (Chic Ill) 47 (1997) 337–340. https://doi.org/10.1093/occmed/47.6.337.

[6] S.Kr. Saha, A. Dutta, P. Ghosh, D. Sukul, P. Banerjee, Novel Schiff-base molecules as efficient corrosion inhibitors for mild steel surface in 1 M HCl medium: experimental and theoretical approach, Physical Chemistry Chemical Physics 18 (2016) 17898–17911. https://doi.org/10.1039/C6CP01993E.

[7] R. Solmaz, Investigation of the inhibition effect of 5-((E)-4-phenylbuta-1,3-dienylideneamino)-1,3,4-thiadiazole-2-thiol Schiff base on mild steel corrosion in hydrochloric acid, Corros Sci 52 (2010) 3321–3330. https://doi.org/10.1016/J.CORSCI.2010.06.001.

[8] N. Vaszilcsin, A. Kellenberger, M.L. Dan, D.A. Duca, V.L. Ordodi, Efficiency of Expired Drugs Used as Corrosion Inhibitors: A Review, Materials 16 (2023) 5555. https://doi.org/10.3390/ma16165555.

[9] M.A. Ahmed, S. Amin, A.A. Mohamed, Current and emerging trends of inorganic, organic and eco-friendly corrosion inhibitors, RSC Adv 14 (2024) 31877–31920. https://doi.org/10.1039/D4RA05662K.
[10] L. Guo, I.B. Obot, X. Zheng, X. Shen, Y. Qiang, S. Kaya, C. Kaya, Theoretical insight into an empirical rule about organic corrosion inhibitors containing nitrogen, oxygen, and sulfur atoms, Appl Surf Sci 406 (2017) 301–306.
[11] H. Assad, A. Kumar, Understanding functional group effect on corrosion inhibition efficiency of selected organic compounds, J Mol Liq 344 (2021) 117755.
[12] D.A. Duca, M.L. Dan, N. Vaszilcsin, Expired Domestic Drug - Paracetamol - as Corrosion Inhibitor for Carbon Steel in Acid Media, in: IOP Conf Ser Mater Sci Eng, Institute of Physics Publishing, 2018. https://doi.org/10.1088/1757-899X/416/1/012043.
[13] M. Bouayed, H. Rabaa, A. Srhiri, J.-Y. Saillard, A. Ben Bachir, A. Le Beuze, Experimental and theoretical study of organic corrosion inhibitors on iron in acidic medium, Corros Sci 41 (1998) 501–517.
[14] M. Abdallah, Antibacterial drugs as corrosion inhibitors for corrosion of aluminium in hydrochloric solution, Corros Sci 46 (2004) 1981–1996.
[15] R.K. Gupta, A. Singh, Pharmaceutical waste recycling for corrosion inhibition applications: A sustainable approach, Sustain Chem Pharm 15 (2020) 100233.
[16] E. McCafferty, Introduction to Corrosion Science, Springer, 2010.
[17] A.A. Al-Amiery, A.A.H. Kadhum, A. Kadihum, A.B. Mohamad, C.K. How, S. Junaedi, Inhibition of mild steel corrosion in sulfuric acid solution by new schiff base, Materials 7 (2014) 787–804. https://doi.org/10.3390/ma7020787.
[18] R. Solmaz, G. Kardaş, M. Çulha, B. Yazıcı, M. Erbil, Investigation of adsorption and inhibitive effect of 2-mercaptothiazoline on corrosion of mild steel in hydrochloric acid media, Electrochim Acta 53 (2008) 5941–5952. https://doi.org/https://doi.org/10.1016/j.electacta.2008.03.055.
[19] M. Özcan, İ. Dehri, M. Erbil, Organic sulphur-containing compounds as corrosion inhibitors for mild steel in acidic media: correlation between inhibition efficiency and chemical structure, Appl Surf Sci 236 (2004) 155–164. https://doi.org/https://doi.org/10.1016/j.apsusc.2004.04.017.
[20] J.-B. Jorcin, M.E. Orazem, N. Pébère, B. Tribollet, CPE analysis by local electrochemical impedance spectroscopy, Electrochim Acta 51 (2006) 1473–1479. https://doi.org/https://doi.org/10.1016/j.electacta.2005.02.128.
[21] A. Popova, M. Christov, S. Raicheva, E. Sokolova, Adsorption and inhibitive properties of benzimidazole derivatives in acid mild steel corrosion, Corros Sci 46 (2004) 1333–1350. https://doi.org/10.1016/j.corsci.2003.09.025.
[22] S. Hari Kumar, S. Karthikeyan, Torsemide and Furosemide as Green Inhibitors for the Corrosion of Mild Steel in Hydrochloric Acid Medium, Ind Eng Chem Res 52 (2013) 7457–7469. https://doi.org/10.1021/ie400815w.
[23] M.A. Amin, S.S. Abd El Rehim, H.T.M. Abdel-Fatah, Electrochemical frequency modulation and inductively coupled plasma atomic emission spectroscopy methods for monitoring corrosion rates and inhibition of low alloy steel corrosion in HCl solutions and a test for validity of the Tafel extrapolation method, Corros Sci 51 (2009) 882–894. https://doi.org/https://doi.org/10.1016/j.corsci.2009.01.006.
[24] Basics of EIS: Electrochemical Research-Impedance Gamry Instruments, (n.d.). https://www.gamry.com/application-notes/EIS/basics-of-electrochemical-impedance-spectroscopy/ (accessed July 6, 2025).
[25] F. Zulkifli, S. Khairina, M.S.M. Ghazali, A.A. Al-Amiery, N. Ismail, V.O. Izionworu, M.J. Suriani, W.B. Wan Nik, Application of electrochemical impedance spectroscopy technology to evaluate passivation performance of film forming and adsorption types corrosion

inhibitors, International Journal of Corrosion and Scale Inhibition 11 (2022) 1303–1318. https://doi.org/10.17675/2305-6894-2022-11-3-23.

[26] E. Jamalizadeh, S.M.A. Hosseini, A.H. Jafari, Quantum chemical studies on corrosion inhibition of some lactones on mild steel in acid media, Corros Sci 51 (2009) 1428–1435. https://doi.org/10.1016/J.CORSCI.2009.03.029.